Experiment 3

X-Ray Diffraction

3.1 The Bragg Picture of Diffraction

X-ray diffraction is the classic example of how elastic scattering of photons can be used to probe periodic structures in condensed matter physics. X-rays (energies from roughly $10keV$ to $50keV$) are used to probe crystal structures because their wavelengths are comparable to atomic spacing in a lattice, and one can then generate interference patterns by reflecting or trasmitting X-rays through the lattice. The simplest picture which is often presented to undergraduates is that of Bragg reflection by parallel planes of atoms in a crystal.

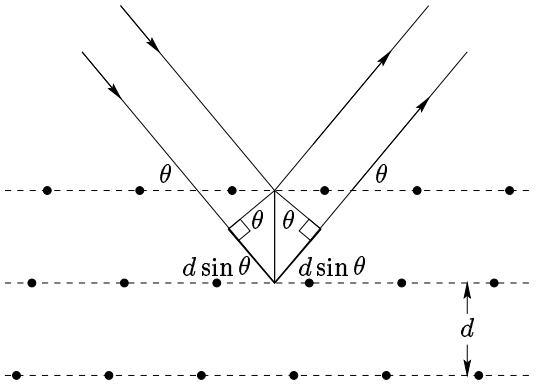

Figure 3.1: Bragg reflection from parallel atomic planes in a crystal lattice.

In this simple picture a beam of radiation is generated at infinity, reflects off of parallel planes and is detected at infinity. If the difference in path length between the two possible reflections is an integral multiple of the X-ray wavelength λ, then constructive interference
occurs at the detector and an intensity maximum will be seen at the special angle θ shown in Fig. 3.1. The Bragg condition can be written as follows:

$$2d\sin\theta = n\lambda \tag{3.1}$$

where d is the spacing between planes and n is an integer.

It is worthwhile mentioning that the discussion presented in this experiment is also applicable to elastic scattering by neutrons and, to a certain degree, electrons. In both of these cases one replaces the wavelength of the X-ray with the deBroglie wavelength of the particle, and the mathematics will be identical. However, in the case of elastic electron scattering one must carefully consider how charge can influence the diffraction pattern.

3.2 The Reciprocal Lattice Picture of Diffraction

The Bragg condition is very easy to visualize, especially when the the diffraction problem can be drawn on a two dimensional page. However, for a real three dimensional crystal lattice the process of identifying planes of atoms and determining how to obtain a diffraction maximum from those planes can be quite complicated. Furthermore, there is no obvious reason why a plane of atoms should provide specular reflection.

Fortunately, there is a mathematical formalism that allows for a more systematic approach to the problem of X-ray diffraction. The idea is to take the Fourier transform a real lattice - the reason being that the electron density in a lattice is periodic, and X-rays are scattered via electron-photon interactions. Consider a three dimensional lattice with a primitive unit cell defined by the vectors $(\vec{a_1},\vec{a_2},\vec{a_3})$. Any point on the lattice can be described by a linear combination of the unit cell vectors, $\vec{r} = u_1\vec{a_1} + u_2\vec{a_2} + u_3\vec{a_3}$, where (u_1, u_2, u_3) are integers. Let the allowed momentum vectors in Fourier space be represented by $\vec{G}$. One can now write a discrete three dimensional Fourier decomposition for the electron density, $n(\vec{r})$.

$$n(\vec{r}) = \sum_{\vec{G}} n_{\vec{G}} e^{i\vec{G}\cdot\vec{r}} \tag{3.2}$$

The set of vectors $\vec{G}$ must satisfy the periodicity of the crystal lattice. For a three dimensional lattice, the allowed vectors $\vec{G}$ can be decomposed into a basis of three vectors, $(\vec{b_1},\vec{b_2},\vec{b_3})$, and these basis vectors must satisfy the following condition:

$$\vec{a_i} \cdot \vec{b_j} = 2\pi\delta_{ij} \tag{3.3}$$

where δ_{ij} is the Kroenecker delta function. This condition ensures that the momentum vectors in any of the three crystal directions have wavelengths that are rational fractions of the lattice spacing in that crystal direction. If one has the set of unit cell vectors $(\vec{a_1},\vec{a_2},\vec{a_3})$, then the vectors $(\vec{b_1},\vec{b_2},\vec{b_3})$ satisfying Eqn. 3.3 can be constructed from the former set of vectors using the following formulae:

$$\begin{aligned}
\vec{b_1} &= 2\pi\frac{\vec{a_2}\times\vec{a_3}}{\vec{a_1}\cdot(\vec{a_2}\times\vec{a_3})} \\
\vec{b_2} &= 2\pi\frac{\vec{a_3}\times\vec{a_1}}{\vec{a_1}\cdot(\vec{a_2}\times\vec{a_3})} \\
\vec{b_3} &= 2\pi\frac{\vec{a_1}\times\vec{a_2}}{\vec{a_1}\cdot(\vec{a_2}\times\vec{a_3})}
\end{aligned} \tag{3.4}$$

The set of vectors $(\vec{b_1},\vec{b_2},\vec{b_3})$ define all possible vectors $\vec{G} = h\vec{b_1} + k\vec{b_2} + l\vec{b_3}$, where (hkl) are integers. Note that these vectors define a lattice upon which all allowed vectors $\vec{G}$ reside, and is referred to as a *reciprocal lattice. It is reccommended that the student determine the reciprocal lattice for a simple cubic structure with a primitive unit cell defined by* $(\vec{a_1}, \vec{a_2}, \vec{a_3}) = (a\hat{x}, a\hat{y}, a\hat{z})$*, where a is a constant.*

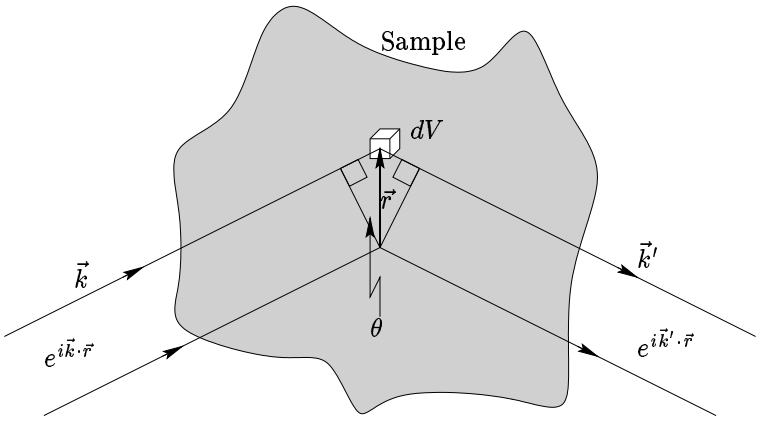

Figure 3.2: A microscopic picture of the scattering of a plane wave by an extended sample.

Now consider a physical description of the scattering process, as depicted in Fig. 3.2. X-rays generated by the source at infinity can be represented as plane waves of the form $e^{i\vec{k}\cdot\vec{r}}$, and the outgoing diffracted waves detected at infinity can also be represented as plane waves of the form $e^{i\vec{k'}\cdot\vec{r}}$. The amplitude of the

diffracted wave will depend upon the *coherent* addition of the reflected waves from all scattering centres throughout the sample. Let this quantity be represented by F.

$$F = \int_{\vec{r}} dV n(\vec{r}) \exp[\imath(\vec{k} - \vec{k'}) \cdot \vec{r}] \tag{3.5}$$

$$F = \sum_{\vec{G}} \int_{\vec{r}} dV n_{\vec{G}} \exp[\imath(\vec{G} + \vec{k} - \vec{k'}) \cdot \vec{r}] \tag{3.6}$$

The intensity of the diffracted wave is given by $|F|^2$, and it will be a maximum if all terms in the integral of Eqn. 3.6 are real. This will occur if the exponent $(\vec{G} + \vec{k} - \vec{k'}) \cdot \vec{r} = 2\pi m$ where m is an integer. However, this statement must hold for *all* allowed values of $\vec{r}$ throughout the sample, and the only way to ensure that is to force $m = 0$.

$$\begin{aligned} (\vec{G} + \vec{k} - \vec{k'}) \cdot \vec{r} &= 0 \\ \vec{G} + \vec{k} - \vec{k'} &= 0 \\ \vec{G} &= \vec{k'} - \vec{k} \end{aligned} \tag{3.7}$$

Therefore, the change in wavevector of the scattered radiation must equal a reciprocal lattice vector in order to provide an intensity maximum in the diffracted wave. One can rewrite Eqn. 3.7 in a more familiar form by noting that for elastic scattering $|\vec{k}| = |\vec{k'}|$ and $|\vec{k}| = 2\pi/\lambda$ for photons. Taking the dot product of Eqn. 3.7 with its self yields

$$\begin{aligned} \vec{G} \cdot \vec{G} &= (\vec{k'} - \vec{k}) \cdot (\vec{k'} - \vec{k}) \\ |\vec{G}|^2 &= 2|\vec{k}|^2 - 2\vec{k} \cdot \vec{k'} \\ &= 4\left(\frac{2\pi}{\lambda}\right)^2 (1 - \cos 2\theta)/2 \\ \lambda &= 2\frac{2\pi}{|\vec{G}|} \sin\theta \end{aligned} \tag{3.8}$$

Upon comparing Eqns. 3.1 and 3.8, one recovers the Bragg condition if $2\pi/|\vec{G}| = d/n$. Therefore, the Bragg formula does have a microscopic justification. Furthermore, if one insists upon placing a physical picture on the reciprocal lattice vectors $\vec{G}$, they are vectors oriented normal to planes of atoms and their magnitudes are inversely proportional to the spacing between the different species of planes.

The reciprocal lattice can be used to predict the existence and positions of diffraction peaks. A convenient means of accomplishing this is called the Ewald construction, and is illustrated for a two dimensional reciprocal lattice in Fig. 3.3.

The incident wavevector is experimentally controlled; its magnitude is inversely proportional to the photon's wavelength and its angle of incidence on the real space lattice dictates its direction in the reciprocal lattice (Eqn. 3.4 can be used to relate the directions of reciprocal lattice vectors to directions in real space). To form the Ewald construction, place the tail of the incident wavevector on any reciprocal lattice site and then draw a sphere of radius $|\vec{k}|$ centred on the head of the incident wavevector. If the sphere intersects any other reciprocal lattice site, then a vector $\vec{G}$ can be drawn between the tail of the incident wavevector $\vec{k}$ and the point of intersection. The vector extending from the point of intersection to the centre of the sphere is then the diffracted wavevector $\vec{k'}$.

3.3 The Reciprocal Lattice of a Powder Sample

Admittedly the reciprocal lattice picture has not made the problem of diffraction from a three dimensional lattice much simpler from an experimentalist's perspective. However, there is a practical trick that can be used which makes the reciprocal lattice picture far more powerful than the Bragg picture; that is to crush the single crystal sample into a powder. By doing so, the sample becomes a collection of a very large number of

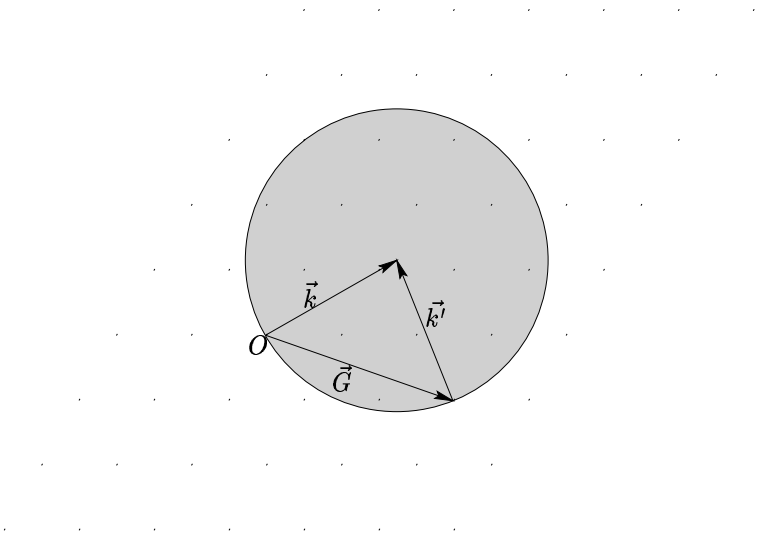

Figure 3.3: The Ewald construction for a two dimensional lattice and an incident wavevector $\vec{k}$.

small samples with no preferred crystallographic orientation- by statistics alone the incident wavevector will inevitably encounter a grain of powder with the correct orientation to cause a diffraction peak. Therefore, the direction of the incident wavevector $\vec{k}$ is irrelevant for powder diffraction. The reciprocal lattice of for a powder sample does not consist of discrete points; rather it is a series of concentric spherical shells of radii $|\vec{G}|$. To picture this, take a reciprocal lattice for a single crystal and rotate it through all possible orientations about $\vec{G} = (0,0,0)$ - each reciprocal lattice point smears out to become a sphere. Now the Ewald construction is easy to satisfy, as shown in Fig. 3.4.

There are two key features to note in Fig. 3.4. First, the picture is invariant if one rotates $\vec{k}$ about the origin. Second, there is only a finite number of reciprocal lattice vectors that can generate diffraction peaks for a given $|\vec{k}|$. Using Eqn. 3.8 and the reciprocal lattice vectors given by Eqn. 3.4, one can calculate all possible Bragg angles for a given crystal structure and photon wavelength. *It is reccommended that the student determine a general formulae for the Bragg angle θ for reciprocal lattice vectors $\vec{G} = h\vec{b_1} + k\vec{b_2} + l\vec{b_3}$ of a simple cubic real space lattice. Express the result in terms of the integers (hkl) and the dimensionless parameter λ/a.*

3.4 The Geometrical Structure Factor

The discussion thusfar is valid for the situation in which there is a single identical atom at each site in a lattice. However, most real materials involve more than one type of element and lattices in which there are clearly inequivalent lattice sites. As an example, consider a face centred cubic (fcc) lattice - it is merely a simple cubic lattice in which the atoms on the corners of the cube are replaced by a four atom structure. If one chooses any corner of the cube as the point (000), then there will be additional atoms at the points $(0, \frac{a}{2}, \frac{a}{2})$, $(\frac{a}{2}, 0, \frac{a}{2})$ and $(\frac{a}{2}, \frac{a}{2}, 0)$. Such a four atom structure is often referred to as a *basis*.

The local electron density at any point in the real space lattice will be a sum of the densities from all of the elements in the basis. For a basis containing j elements at locations $\vec{r_j}$,

$$n(\vec{r}) = \sum_j n_j(\vec{r} - \vec{r_j}) \tag{3.9}$$

This addtional structure will alter the Fourier transform of the electronic density, thereby necessitating a rewriting of Eqn. 3.6. Begin by examining Eqn. 3.5 for a diffraction maximum; in that situation there is only one relevant vector $\vec{G_{hkl}} = \vec{k'} - \vec{k}$ and every unit cell in the crystal will be interacting with the incident radiation in an identical manner. Therefore, one can replace the difference in wavevectors with $\vec{G_{hkl}}$ and

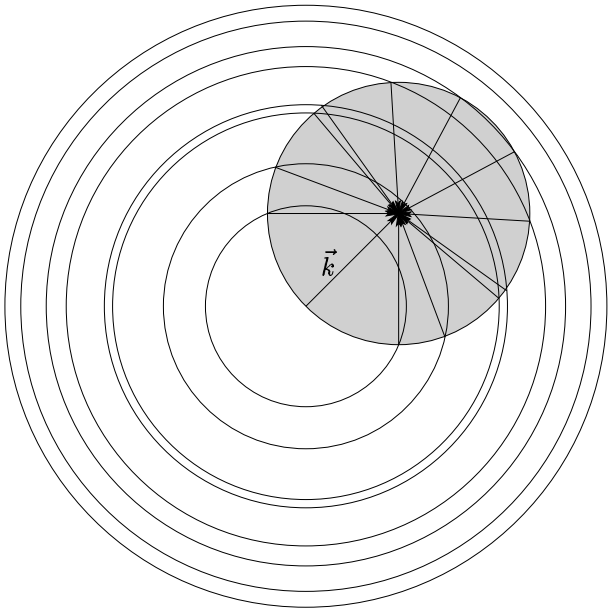

Figure 3.4: The reciprocal lattice of a powder sample and the Ewald construction for an incident wavevector $\vec{k}$. Note that the picture is identical for all orientations of $\vec{k}$.

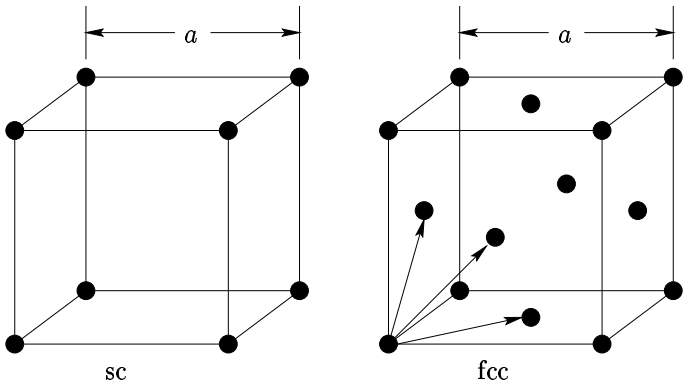

Figure 3.5: A picture of a simple cubic and face centred cubic lattice. One can generate the fcc lattice from a sc lattice by replacing each atom in the sc lattice with a four atom (tetrahedral) structure.

restrict the integral to being over a single primitive unit cell of the real space lattice. If there are N primitive unit cells in the sample, then the diffraction amplitude can be written as follows:

$$\begin{aligned} F_{hkl} &= N \int_{\text{unit cell}} dV\, n(\vec{r}) \exp[-\imath \vec{G_{hkl}} \cdot \vec{r}] \\ &= N \sum_j \exp[-\imath \vec{G_{hkl}} \cdot \vec{r_j}] \int_{\text{unit cell}} dV\, n_j(\vec{\rho}) \exp[-\imath \vec{G_{hkl}} \cdot \vec{\rho}] \\ &= N \sum_j f_j \exp[-\imath \vec{G_{hkl}} \cdot \vec{r_j}] \end{aligned} \tag{3.10}$$

where $\vec{\rho} = \vec{r} - \vec{r_j}$ and f_j captures the details of the local electronic structure around each of the j atoms in the basis. The quantity f_j is called an *atomic form factor.*

$$f_j = \int_{\text{unit cell}} dV\, n_j(\vec{\rho}) \exp[-\imath \vec{G_{hkl}} \cdot \vec{\rho}] \tag{3.11}$$

Examine and compare Eqns. 3.6 and 3.10 carefully; if one evaluates Eqn. 3.6 for only a particular $\vec{G_{hkl}}$ (neglect the sum over all $\vec{G}$), then one will obtain $F = \int_{\vec{r}} dV\, n_{\vec{G_{hkl}}}$, which is a purely real quantity. However, with the inclusion of a basis there are additional complex coherence factors and real atomic form factors in Eqn. 3.10.

It is convenient to rewrite Eqn. 3.10 in terms of the vector components of $\vec{G_{hkl}} = h\vec{b_1} + k\vec{b_2} + l\vec{b_3}$ and $\vec{r_j} = x_j\vec{a_1} + y_j\vec{a_2} + z_j\vec{a_3}$. This quantity is referred to as a *structure factor* for a particular basis.

$$\begin{aligned} S_{hkl} &= \sum_j f_j \exp[-\imath \vec{G_{hkl}} \cdot \vec{r_j}] \\ &= \sum_j f_j \exp[-\imath 2\pi(hx_j + ky_j + lz_j)] \end{aligned} \tag{3.12}$$

It is important to note that S_{hkl} can be zero for particular sets of integers (hkl) in some bases. Therefore, even if the Bragg condition can be met for a particular plane of atoms, the intensity maximum can be nulled by interference effects arising from the structure factor. *It is reccommended that the student evaluate S_{hkl} for a fcc lattice. Determine the the four shortest reciprocal lattice vectors $\vec{G}$ which generate nonzero values of S_{hkl} and then calculate the Bragg angle θ for these $\vec{G}$. To begin, take the vectors* $(0,0,0)$, $(0,\frac{a}{2},\frac{a}{2})$, $(\frac{a}{2},0,\frac{a}{2})$ *and* $(\frac{a}{2},\frac{a}{2},0)$ *and rewrite them in terms of the sc lattice vectors as* $\vec{r_j} = x_j\vec{a_1} + y_j\vec{a_2} + z_j\vec{a_3}$.

3.5 The AMPEL *Rigaku 300* X-Ray Facility

The X-ray apparatus is located in the AMPEL building, room 349. It is classified as a communal user facility and is an essential component of many research programs. The students of Physics 409 have been given access to this facility by the good graces of the researchers in AMPEL. Please be extremely careful with this apparatus so that we may continue to be welcome in the future.

The *Rigaku model 300* Rotating Anode X-Ray apparatus is a fully automated system for performing X-ray diffraction on both single crystals and powder samples. The apparatus is rapidly approaching 20 years of age, but is very representative of the best X-ray facilities available in the world today. However, it is far more important for the student to understand the physics behind the measurement procedure than to know the sequence of knobs and buttons that need to be twiddled in order to make a measurement with this particular apparatus. Therefore, there will be very few specifics presented in this manual. A schematic diagram of the apparatus is presented in Fig. 3.6.

3.5.1 X-Ray Generation

The *Rigaku* apparatus generates X-rays by bombarding a copper target held in vacuum with high energy electrons, typically $20 \rightarrow 100\ keV$. Electrons are ejected from a heated filament and accelerated towards the

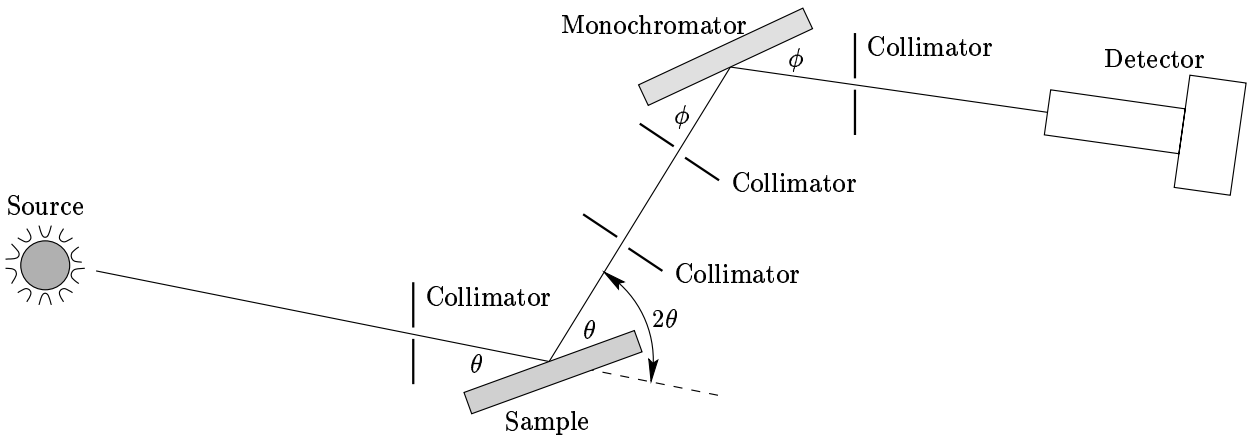

Figure 3.6: The schematic layout of the *Rigaku model 300* apparatus. Shown are the principle components (source, sample, monochromator, detector and collimators) and the relevant angles (Bragg angles for the sample and graphite monochromator, θ and ϕ, respectively).

target by the high voltage. A fraction of these ballistic electrons knock out inner core electrons of the target atoms, and then bound electrons at higher energies cascade through the atomic orbitals, thereby generating a shower of photons at discrete energies. The relevant photons for this experiment are generated by the following atomic transitions:

$$K_{\alpha_1} \qquad 2p_{3/2} \mapsto 1s_{1/2}, \lambda = 1.540598\,\mathring{A}$$

$$K_{\alpha_2} \qquad 2p_{1/2} \mapsto 1s_{1/2}, \lambda = 1.544418\,\mathring{A}$$

Ideally, there would only be a single X-ray used in an experiment, but the K_α spectral lines are so close that they cannot be separated easily. Fortunately, it is known that the K_{α_1} line is twice as intense as K_{α_2}, so it is possible to separate their effects numerically during analysis of diffraction data.

A key practical problem with X-ray generation by this means is the intense heating of the sample. This is handled by sinking as much heat as possible into a water cooling system and by rotating the target to distribute the heat load.

3.5.2 The $\theta/2\theta$ Scans

The Ewald construction in Fig. 3.4 suggests that it is a very simple process to obtain diffraction peaks from a powder sample; by applying a collimated beam of X-rays to a powder the Bragg condition will be met for several types of atomic planes simultaneously, and the diffraction peaks can be found by scanning the detector over an arc from $0 \rightarrow 180^o$ with respect to the direction of the incident wavevector. This method would work for cylindrically symmetric samples, but in many cases it is far more convenient and advantageous to work with planar samples. The intensity of the signal can be optimized by always maintaining specular reflection from the surface of a planar sample. This can be accomplished by rotating the sample surface by the Bragg angle θ with respect to the incident wavevector $\vec{k}$ and the detector by an angle 2θ with respect to $\vec{k}$, as indicated in Fig. 3.6. This type of geometry is referred to as a $\theta/2\theta$ *scan*, in which the sample and detector are moved by synchronized stepper motors while the X-ray source is kept fixed.

3.5.3 Monochromator and Detector

The incident beam will have many photon energies, but only the K_α lines have the correct wavelengths for performing X-ray diffraction. To filter out the undesirable wavelengths a piece of highly crystalline pyrolytic graphite is used as a monochromator. The specular reflection from the monochromator is arranged such

that the angle ϕ matches the Bragg condition for $(hkl) = (001)$ reflections from the graphite if $\lambda \approx 1.54\,\mathring{A}$. Finally, the K_α radiation is detected by a conventional silicon detector operating at room temperature.

3.5.4 Collimating Slits

Collimating slits are placed at one point along each of the three axes of the diffractometer. A vertical slit $1\,mm \times 2\,cm$ is placed before the sample, and other slits of similar dimensions are placed before the monochromator and detector. Narrower slits allow for better angular resolution, but significantly decrease the measured count rates.

3.6 Samples and Data Analysis

Powder samples are commonly used not only because it is relatively simple to find the diffraction intensity peaks, but because powders are often an intermediate in the production of technologically important materials. However, powder samples can be very messy, for they have to be packed tightly into glass receptacles and can fall out during experiments. Therefore, in the interest of saving time and avoiding frustration, polycrystalline samples of aluminum and copper will be used for this experiment - all of the physics is identical to what has been presented for powders, but the samples can be a single piece of solid. Pieces of 1/8" thick Al and Cu metal from any machine shop will suffice because industrially fabricated metals are always polycrystalline.

Both Al and Cu have fcc lattice structures, hence the calculations that were suggested throughout this manual will be essential for the data analysis. The *Rigaku* software outputs an ASCII file of counts/sec vs. angle, which can be imported into graphing software or Mathematica for analysis. To process the data, compare the angular positions of the Bragg peaks to the formulae that have been derived for a fcc lattice and one should be able to determine the lattice constant a. For the more ambitious, it is possible to separate the K_{α_1} and K_{α_2} diffraction patterns by modelling the spectral lines as Lorentzians (with the 2:1 intensity mentioned previously) convoluted with a Gaussian to represent the randomn distribution of Bragg planes.

3.7 Selected References

C. Kittel, Introduction to Solid State Physics. John Wiley and Sons, Inc., Toronto, Sixth Edition (1986)

If you are unfamiliar with crystal structure and the language of crystallography, then I reccommend reading Chapter 1 of this book. Kittel also presents a very lucid derivation of diffraction in a reciprocal lattice picture in Chapter 2, and I have chosen to follow his notation in this manual. However, the author neglected to discuss powder methods, despite the frequent use of powder diffraction data in the book.

N.W. Ascroft and N.D. Mermin, Solid State Physics. W.B. Saunders Company, Philadelphia, USA (1976)

This is generally the choice of condensed matter textbook for experimentalists. It gives an introduction to the many ways of performing X-ray diffraction in Chapter 6, but fails to provide a clear theoretical picture of the phenomenon.

Rigaku Model 300 Operator's Manual

Please ask the teaching assistant if you wish to borrow a copy of the manual. The manual contains purely technical details.

3.8 ****SAFETY ISSUES****

Unlike most undergraduate experiments that have been declawed, detoothed and tamed for your safety, the high intensity X-ray source in this experiment is a *very serious* and *very real* health hazard. Keep in mind that this is an apparatus designed to be used by experts who are fully aware of the health hazards associated with X-ray radiation - therefore be very cautious and think through your every motion when the X-ray source is activated. DO NOT even attempt to open the leaded plexiglass shields surrounding the device if the shutter in front of the source is not closed or you cannot visually confirm that it is closed. This device

is capable of leaving permanent damage (severe burns, scarring, cancer, blindness) with only a few seconds of exposure to your body.